Alignment of transmembrane regions in the cystic fibrosis transmembrane conductance regulator chloride channel pore

Wuyang Wang, Yassine El Hiani, and Paul Linsdell

Department of Physiology and Biophysics, Dalhousie University, Halifax, Nova Scotia B3H 1X5, Canada

Different transmembrane (TM) α helices are known to line the pore of the cystic fibrosis TM conductance regulator (CFTR) Cl^- channel. However, the relative alignment of these TMs in the three-dimensional structure of the pore is not known. We have used patch-clamp recording to investigate the accessibility of cytoplasmically applied cysteine-reactive reagents to cysteines introduced along the length of the pore-lining first TM (TM1) of a cysteineless variant of CFTR. We find that methanethiosulfonate (MTS) reagents irreversibly modify cysteines substituted for TM1 residues K95, Q98, P99, and L102 when applied to the cytoplasmic side of open channels. Residues closer to the intracellular end of TM1 (Y84–T94) were not apparently modified by MTS reagents, suggesting that this part of TM1 does not line the pore. None of the internal MTS reagent-reactive cysteines was modified by extracellular [2-(trimethylammonium)ethyl] MTS. Only K95C, closest to the putative intracellular end of TM1, was apparently modified by intracellular [2-sulfonatoethyl] MTS before channel activation. Comparison of these results with recent work on CFTR-TM6 suggests a relative alignment of these two important TMs along the axis of the pore. This alignment was tested experimentally by formation of disulfide bridges between pairs of cysteines introduced into these two TMs. Currents carried by the double mutants K95C/I344C and Q98C/I344C, but not by the corresponding single-site mutants, were inhibited by the oxidizing agent copper(II)-*o*-phenanthroline. This inhibition was irreversible on washing but could be reversed by the reducing agent dithiothreitol, suggesting disulfide bond formation between the introduced cysteine side chains. These results allow us to develop a model of the relative positions, functional contributions, and alignment of two important TMs lining the CFTR pore. Such functional information is necessary to understand and interpret the three-dimensional structure of the pore.

INTRODUCTION

Cystic fibrosis is caused by genetic mutations that disrupt the function of the CFTR, an anion channel expressed predominantly in epithelial cells (Rowe et al., 2005). CFTR is a member of the ATP-binding cassette (ABC) family of membrane transport proteins, but is unique within this family in acting as an ion channel rather than an active transporter (Gadsby et al., 2006). As with other ABC proteins, CFTR has a modular architecture consisting of two groups of six transmembrane (TM) α helices, each followed by a cytoplasmic nucleotide–binding domain. In CFTR, these two homologous halves of the molecule are connected by a unique cytoplasmic regulatory domain. The TMs, nucleotide binding, and regulatory domains are the sites of TM anion movement, control of channel gating by intracellular ATP, and channel regulation by phosphorylation and dephosphorylation, respectively (Kidd et al., 2004; Gadsby et al., 2006).

To understand CFTR's role as an anion channel, it is important to understand the structure and function of the TM permeation pathway through which anions move. Indeed, the CFTR pore region has been investigated using a combination of imaging (Mio et al., 2008; Zhang et al., 2009), functional (Kidd et al., 2004; Linsdell, 2006), and molecular modeling (Mornon et al., 2008; Serohijos et al., 2008; Alexander et al., 2009) studies. Functional evidence suggests that individual TM regions 1, 5, 6, 11, and 12 all make some contribution to the lining of the pore (McCarty, 2000; St. Aubin and Linsdell, 2006; Linsdell, 2006; Mornon et al., 2008; Fatehi and Linsdell, 2009; Zhou et al., 2010), with TMs 1 and 6 being particularly important to the functional properties of the central/outer part of the pore (Ge et al., 2004). The relative positions of different TMs can be observed in atomic models of the CFTR protein that are based on homology modeling of the bacterial ABC protein Sav1866 (Mornon et al., 2008; Serohijos et al., 2008). However, there is little functional or direct imaging evidence to support the overall arrangement or alignment of the TMs around the pore, although limited TM cross-linking experiments have been used to demonstrate physical proximity of specific amino acid

Correspondence to Paul Linsdell: paul.linsdell@dal.ca

Abbreviations used in this paper: ABC, ATP-binding cassette; BHK, baby hamster kidney; CuPhe, copper(II)-*o*-phenanthroline; DTT, dithiothreitol; MTS, methanethiosulfonate; MTSES, [2-sulfonatoethyl] MTS; MTSET, [2-(trimethylammonium)ethyl] MTS; PPi, pyrophosphate; TM, transmembrane.

The Rockefeller University Press $30.00
J. Gen. Physiol. Vol. 138 No. 2 165–178
www.jgp.org/cgi/doi/10.1085/jgp.201110605

residues in TMs 6 and 12 (Chen et al., 2004), TMs 6 and 7 (Wang et al., 2007), and TMs 1 and 12 (Zhou et al., 2010). As a result, current understanding of functionally important parts of the pore is limited to two-dimensional rather than three-dimensional models. For example, the narrow region of the pore that might form a "selectivity filter" that discriminates between Cl^- and other anions is thought to be lined by TM6 residues F337 and T338 (Linsdell, 2006), but residues from other TMs contributing to this region have not been identified. We recently suggested that TM6 residues I344 and V345 might be located around a "barrier" that prevents anion movement in nonactivated CFTR channels (El Hiani and Linsdell, 2010), but again, residues from other TMs that might contribute to such a barrier have not been identified. The outer mouth of the CFTR pore is thought to be decorated by positively charged amino acid side chains coming from different TM regions or the short extracellular loops that connect the TMs (Zhou et al., 2008), but the relative location and depth into the pore from the outside of different positively charged side chains have not been reported. A further impediment to fully understanding the structure of the pore is that only one TM, TM6, has been probed using cysteine scanning mutagenesis and application of cysteine-reactive probes to both the intracellular and extracellular side of the membrane (Cheung and Akabas, 1996; Beck et al., 2008; Alexander et al., 2009; Bai et al., 2010; El Hiani and Linsdell, 2010), allowing the contribution of the entire length of this TM region to the pore to be ascertained.

We have studied the accessibility of amino acid residues in TM1, known to be functionally important in the CFTR pore (Akabas et al., 1994; Ge et al., 2004; Linsdell, 2006), to substances applied from either side of the membrane. We find that cysteine-reactive substances have access to a restricted region in the outer part of TM1, depending on the side of the membrane to which they are applied. Comparison of the functional effects of modification of cysteines introduced into TM1 with those observed for cysteines in TM6 suggest a relative alignment of these two TMs, which we confirm using disulfide cross-linking of cysteine side chains introduced into these two TMs. These results allow us to develop a functional model of the pore that incorporates three-dimensional information relating to two important pore-lining TMs.

MATERIALS AND METHODS

Experiments were performed using baby hamster kidney (BHK) cells transiently transfected with human CFTR. As in our recent study on CFTR-TM6 (El Hiani and Linsdell, 2010), we have used a human CFTR variant in which all 18 endogenous cysteine residues had been substituted by other amino acids (as described in Mense et al., 2006), and which also includes a mutation in the first nucleotide-binding domain (V510A) to increase protein expression in the cell membrane (Li et al., 2009). In this background (referred to as "cys-less CFTR"), we have mutated individually 21 consecutive amino acids in TM1, from Y84 at the putative cytoplasmic end to R104 at the extracellular end, to cysteine. Mutagenesis was performed using the QuikChange site-directed mutagenesis system (Agilent Technologies) and verified by DNA sequencing. All constructs used were in the pIRES2-EGFP vector (Li et al., 2009), allowing coexpression of CFTR with enhanced green fluorescent protein. BHK cells were transiently transfected as described previously (Gong et al., 2002), except that 24 h after transfection, cells were transferred to 27°C to promote mature protein expression (Li et al., 2009). Cells were used for electrophysiological experimentation after 1–3 d at 27°C. Individual cells were selected for patch-clamp investigation based on identification of enhanced green fluorescent protein expression by fluorescence microscopy.

Macroscopic CFTR currents were recorded using patch-clamp recording from inside-out membrane patches excised from BHK cells as described in detail previously (Linsdell and Hanrahan, 1996; Linsdell and Gong, 2002). After patch excision, any pretreatment of the inside-out patch if necessary (see below), and recording of background currents, CFTR channels were activated by exposure to 20 nM PKA catalytic subunit plus 1 mM MgATP in the cytoplasmic solution. Unless stated otherwise, CFTR channel activity was then further increased by the addition of 2 mM of sodium pyrophosphate (PPi). PPi was used to maximize and stabilize macroscopic current amplitude, which was very small for many TM1 mutants, and so increase resolution. Both intracellular (bath) and extracellular (pipette) solutions contained 150 mM NaCl, 2 mM $MgCl_2$, and 10 mM *N*-tris(hydroxymethyl)methyl-2-aminoethanesulfonate (pH adjusted to 7.4 using NaOH). Channels were exposed to intracellular and extracellular cysteine-reactive methanethiosulfonate (MTS) reagents to covalently modify introduced cysteine side chains. Two MTS reagents, the positively charged [2-(trimethylammonium)ethyl] MTS (MTSET) and the negatively charged [2-sulfonatoethyl] MTS (MTSES), were used. These reagents were initially prepared as high concentration (160-mM) stock solutions in distilled water and stored frozen as small-volume aliquots until the time of use, when they were diluted in bath solution and used immediately. The oxidizing agent copper(II)-*o*-phenanthroline (CuPhe) was prepared freshly before each experiment by mixing $CuSO_4$ (200 mM in distilled water) with 1,10-phenanthroline (200 mM in ethanol) in a 1:4 molar ratio, and used at a final concentration of 100 µM Cu^{2+} and 400 µM phenanthroline.

Initially high concentrations of MTS reagents (200 µM MTSES or 2 mM MTSET) that have previously been found to be without effect on cys-less CFTR currents (Li et al., 2009; El Hiani and Linsdell, 2010; Zhou et al., 2010) were applied to the cytoplasmic face of inside-out membrane patches after maximal channel activation, and currents were monitored for at least 5 min until the current had again reached a steady amplitude (see Fig. 1 A). To measure the rate of modification of open channels (see Fig. 3), macroscopic current amplitude was monitored continuously, and the time-dependent change in amplitude after the addition of MTSES was fitted by a single-exponential function. To ensure that differences in the modification rate between different MTS reagents did not reflect differences in the voltage dependence of MTS reagent entry into the pore, the membrane patch was held at 0-mV membrane potential, and current amplitude was monitored during brief voltage deflections (see below for details of voltage-clamp protocols used). In cases where the rate of modification was very fast, the concentration of MTS reagents used was reduced (to 20 µM MTSES or 200 µM MTSET). The time constant of exponential current decay, τ, was used to calculate the apparent second-order reaction rate constant, k, from the equation $k = 1 / ([MTS]\ \tau)$.

In some cases, MTS reagents were used to pretreat intact cells (external application; Fig. 4) or inside-out membrane patches (internal application; Fig. 5) before recordings. In Fig. 4, channels were pretreated with external MTSET. Intact cells were preincubated in 5 mM MTSET (in normal bath solution) for 5 min, after which cells were washed thoroughly with bath solution and transferred to the recording chamber for patch-clamp analysis. MTSET was used in these experiments, as we have previously found it to be a less state-dependent probe of the outer pore than MTSES (Fatehi and Linsdell, 2008). Indeed, we have previously used a similar MTSET pretreatment protocol to identify positively several externally accessible sites in CFTR (Zhou et al., 2008; Fatehi and Linsdell, 2009; El Hiani and Linsdell, 2010), including R104 at the external end of TM1 (Zhou et al., 2008).

In Fig. 5, channels were pretreated with internal MTSES, using one of two pretreatment protocols described previously (El Hiani and Linsdell, 2010). After patch excision to the inside-out configuration, 200 µM MTSES was added to the cytoplasmic (bath) solution. MTSES was applied alone (for modification of nonactivated channels) (Fig. 5 B) or together with 20 nM PKA and 1 mM ATP (for modification of activated channels) (Fig. 5 A). After a 2-min treatment period, all substances were washed from the bath using normal bath solution. After recording of background leak currents, CFTR channels were then activated using 20 nM PKA, 1 mM ATP, and 2 mM PPi, as usual, and then exposed to a test treatment of MTSES. Although this approach does not quantify the rate of modification of nonactivated channels, it does provide a simple separation of side chains that are readily modified in nonactivated channels versus those for which the rate of modification in nonactivated channels is negligible (see El Hiani and Linsdell, 2010). Pretreatment for 2 min with 200 µM MTSES is expected to result in ~100% modification in fully activated channels (see Fig. 3 B). A similar approach was used to pretreat channels with CuPhe in Fig. 7; in these experiments, the degree of cross-linking induced by CuPhe during the pretreatment period was quantified by the effects of 5 mM dithiothreitol (DTT) applied after washing and subsequent channel activation with PKA and ATP.

For channel inhibition by Cu^{2+} ions, concentration–inhibition relationships (Fig. 8 B) were fitted by an equation of the form:

$$\text{Fractional unblocked current} = 1 \,/\, \left(1 + \left[Cu^{2+}\right] \,/\, K_d\right)^{nH},$$

where K_d is the apparent inhibitor dissociation constant, and nH is the slope factor or Hill coefficient.

Current traces were filtered at 100 Hz using an eight-pole Bessel filter, digitized at 250 Hz, and analyzed using pCLAMP-10 software (Molecular Devices). Macroscopic I-V relationships were constructed using depolarizing ramp protocols (Linsdell and Hanrahan, 1998) from a holding potential of 0 mV. Background (leak) currents recorded before the addition of PKA and ATP have been subtracted digitally, leaving uncontaminated CFTR currents (Linsdell and Hanrahan, 1998; Gong and Linsdell, 2003).

Experiments were performed at room temperature (21–24°C). Values are presented as mean ± SEM. Tests of significance were performed using a Student's two-tailed *t* test, unless stated otherwise. All chemicals were from Sigma-Aldrich, except for PKA (Promega) and MTSES and MTSET (Toronto Research Chemicals).

Online supplemental material

Fig. S1 shows macroscopic I-V relationships and lack of MTS reagent sensitivity for 15 different mutants studied. Fig. S2 shows the lack of sensitivity to the reducing agent DTT of macroscopic currents carried by the double-cysteine mutant channels K95C/I344C and Q98C/I344C. Fig. S3 shows the predicted locations of cross-linked residues in a current homology model of the CFTR membrane–spanning domain. Figs. S1–S3 are available at http://www.jgp.org/cgi/content/full/jgp.201110605/DC1.

RESULTS

Accessibility of cysteines introduced into TM1

We (El Hiani and Linsdell, 2010) and others (Bai et al., 2010) have recently used internal application of MTS reagents to identify pore-lining cysteine side chains introduced into TM6 of cys-less CFTR. In the present study, we used a similar approach to identify pore-lining side chains in TM1. Using site-directed mutagenesis, we substituted cysteines for each of 21 consecutive amino acids, from Y84 near the putative intracellular end of TM1 to R104 near the extracellular end, in a V510A cys-less background (see Materials and methods). In most cases, expression of these mutants in BHK cells led to the appearance of macroscopic PKA- and ATP-dependent currents in inside-out membrane patches (e.g., Figs. 1 and S1). The one exception was E92C, which failed to generate any measureable current, even after multiple attempts with two independently constructed mutant cDNAs. Substitution of E92 by other residues in a wild-type CFTR background also fails to yield functional channels in mammalian cells (unpublished data).

The application of negatively charged MTSES (200 µM) or positively charged MTSET (2 mM) to the intracellular solution after channel activation with PKA, ATP, and PPi had no significant effect on macroscopic current amplitude in cys-less CFTR (Fig. 1, A and B), as reported previously (El Hiani and Linsdell, 2010; Zhou et al., 2010), although higher concentrations of MTSES do cause a reversible, voltage-dependent inhibition under these conditions (Li et al., 2009). A similar lack of effect after prolonged (>5-min) exposure to such high concentrations of both MTSES and MTSET was observed in 16 out of 20 cysteine-substituted mutants tested (Figs. 1 B, 2, and S1), suggesting that the side chains at these positions are not accessible to internal MTS reagents. This list of MTS reagent–insensitive mutants includes R104C (Figs. 1 B and 2), which we have previously shown to be sensitive to modification by externally applied MTSES and MTSET (Zhou et al., 2008). In contrast, macroscopic currents carried by four mutants, K95C, Q98C, P99C, and L102C, were found to be significantly and rapidly sensitive to the application of both MTSES and MTSET (Figs. 1–3). In each case, macroscopic current amplitude was decreased by the application of MTSES but increased by MTSET (Figs. 1 and 2), a pattern also frequently observed for cysteines introduced into TM6 (Bai et al., 2010; El Hiani and Linsdell, 2010). These effects of MTS reagents were not reversed by washing the reagents from the bath (see also Fig. 5 C). However, as previously described for cysteines introduced into TM6

(El Hiani and Linsdell, 2010), the effects of MTS reagents could be reversed by the addition of 2–5 mM DTT. The effects of MTS reagents on the amplitude of macroscopic currents carried by different channel constructs are summarized in Fig. 2.

For those four mutants that were sensitive to modification by MTS reagents, the rate of modification was estimated from the time course of macroscopic current amplitude change after the application of MTSES (20–200 µM) or MTSET (200 µM–2 mM). As shown in Fig. 3 A, MTSES modification was rapid in K95C, even when a low concentration of MTSES (20 µM) was used, and considerably slower in L102C (using 200 µM MTSES). The overall pattern of calculated modification rate

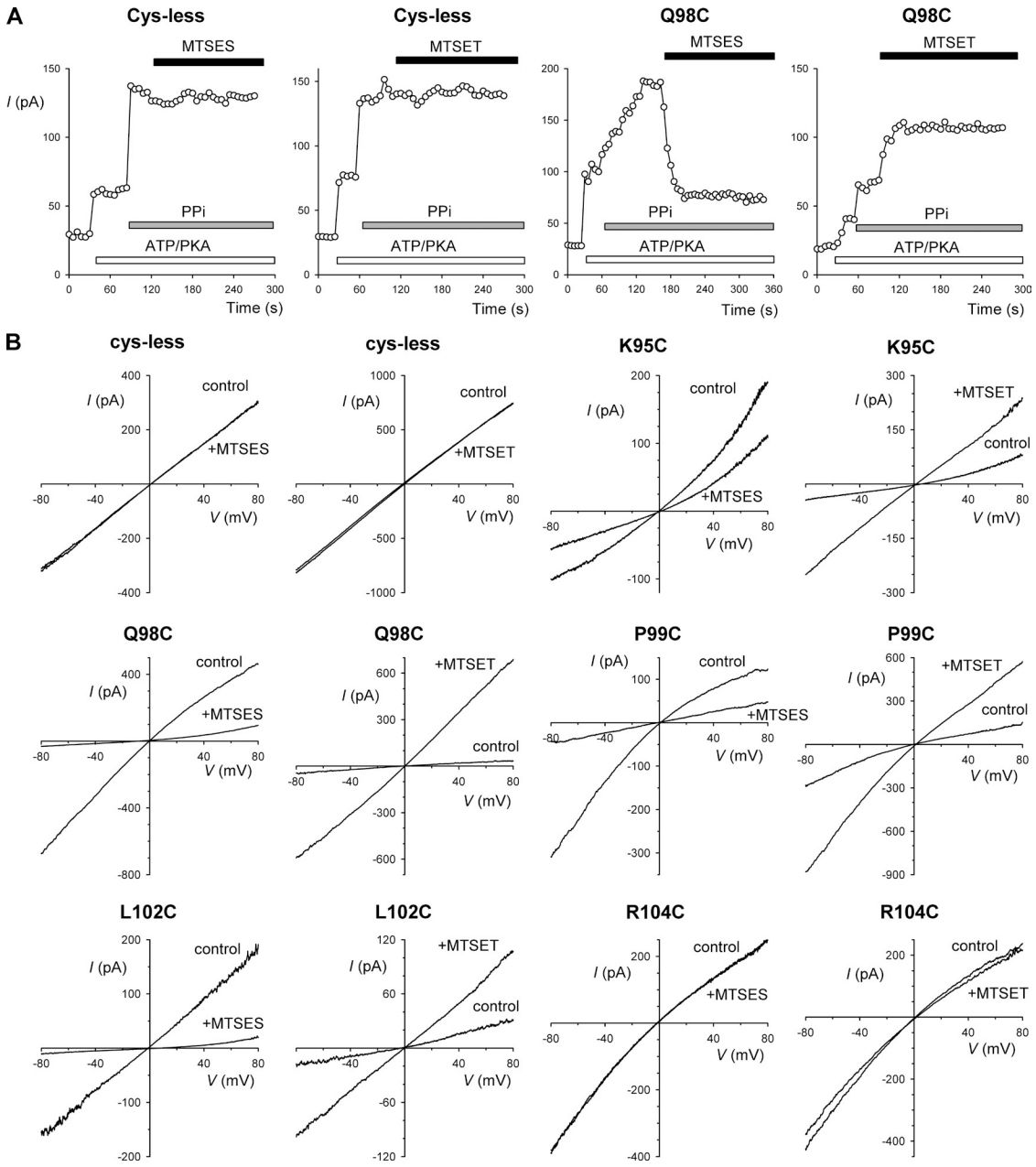

Figure 1. Modification of cysteine-substituted CFTR-TM1 mutants by internal MTS reagents. (A) Example time courses of macroscopic currents (measured at +50 mV) carried by cys-less CFTR and Q98C inside-out membrane patches. After patch excision and recording of baseline currents, patches were treated sequentially with 20 nM PKA and 1 mM ATP, 2 mM PPi, and either 200 µM MTSES or 2 mM MTSET. Note that whereas these MTS reagents have no effect on cys-less CFTR current amplitude, they cause rapid inhibition (MTSES) or augmentation (MTSET) of current carried by Q98C. (B) Example leak-subtracted I-V relationships for cys-less CFTR, K95C, Q98C, P99C, L102C, and R104C, recorded from inside-out membrane patches after maximal channel activation with 20 nM PKA, 1 mM ATP, and 2 mM PPi. In each panel, currents recorded before the application of MTS reagents (control) and after full modification by 200 µM of intracellular MTSES or 2 mM MTSET had been achieved.

constants was that modification was faster for cysteines introduced closer to the intracellular end of TM1, and slower for cysteines located more deeply along the axis of TM1 (Fig. 3 B). This same pattern was observed both for the inhibition of current amplitude caused by MTSES application and the increase in current amplitude after MTSET application (Fig. 3 B). Interestingly, the rate of modification by MTSET was consistently lower than that by MTSES, with the MTSET modification rate constant being between 8- and 13-fold lower for all MTS-sensitive mutants studied (Fig. 3 B).

Side and state dependence of modification

MTS reagents are not permeant in CFTR (Beck et al., 2008; Alexander et al., 2009; El Hiani and Linsdell, 2010); however, we previously identified three sites in TM6 at which introduced cysteines could be modified by both internally and externally applied MTS reagents (El Hiani and Linsdell, 2010). To gain some information on the orientation of TM1 in the CFTR pore, we therefore examined whether cysteines introduced into TM1 that were sensitive to modification by intracellular MTS reagents could also be modified by extracellular MTSET. Using a similar approach to that used previously in TM6 (El Hiani and Linsdell, 2010), we sought to identify sites at which pretreatment with externally applied MTSET would prevent subsequent modification by internally applied MTSET. As described previously (El Hiani and Linsdell, 2010), intact cells were exposed to a high concentration of MTSET (5 mM) for 5 min. Cells were then washed and transferred to the experimental chamber for patch-clamp analysis. After patch excision to the inside-out configuration, CFTR channels were activated using PKA, ATP, and PPi and subsequently treated with intracellular MTSET (2 mM), exactly as in Fig. 1. As shown in Fig. 4 A, patches excised from MTSET-pretreated cells expressing K95C, Q98C, P99C, or L102C all gave macroscopic currents that were increased in amplitude after the addition of 2 mM

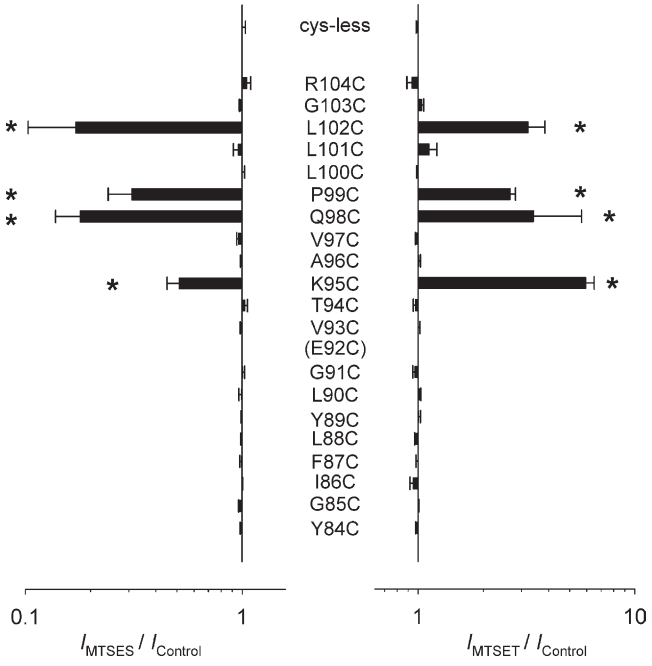

Figure 2. Effects of internal MTS reagents on cysteine-substituted CFTR-TM1 mutants. Mean effect of treatment with 200 µM MTSES (left) or 2 mM MTSET (right) on macroscopic current amplitude in cys-less CFTR and in each of 20 different cysteine-substituted TM1 mutants. Note that no currents were recorded from patches excised from cells transfected with E92C cDNA (see Results). Effects of these two MTS reagents were quantified by measuring current amplitudes at membrane potentials of +80 mV (for MTSES, left) and −80 mV (for MTSET, right) before MTS reagent application and after complete modification had taken place. Mean of data from three to nine patches. Asterisks indicate a significant difference from cys-less ($P < 0.05$).

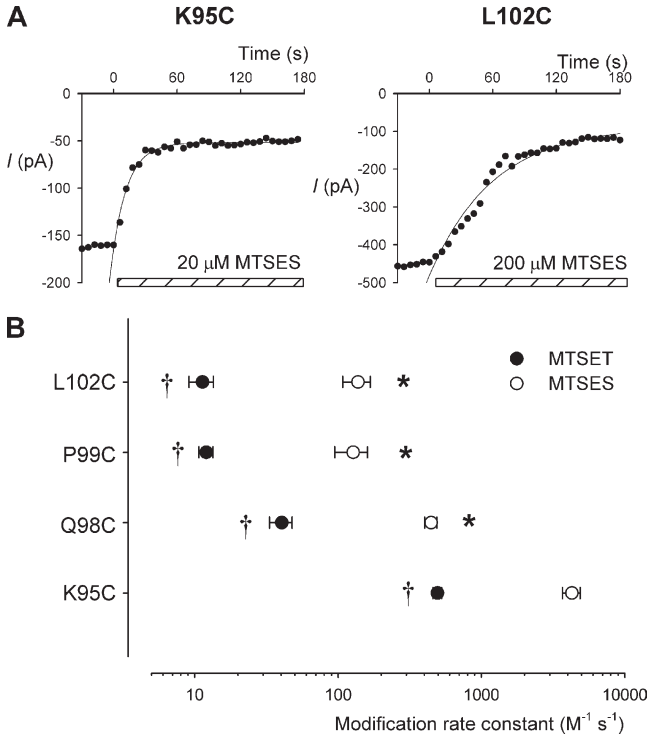

Figure 3. Time course of modification by MTSES and MTSET. (A) Example time courses of macroscopic currents (measured at −50 mV during brief voltage excursions from a holding potential of 0 mV) carried by K95C (left) and L102C (right) as indicated, in inside-out membrane patches. Current amplitudes were measured every 6 s after the attainment of stable current amplitude after channel activation with 20 nM PKA, 1 mM ATP, and 2 mM PPi. In each case, MTSES (20 µM for K95C and 200 µM for L102C) was applied to the cytoplasmic face of the patch at time zero (as indicated by the hatched bar at the bottom of each panel). The decline in current amplitude after MTSES application has been fitted by a single-exponential function in each case. (B) Calculated modification rate constants for both MTSES (○) and MTSET (●) for each of the four MTS reagent–sensitive mutants listed. Asterisks indicate a significant difference from MTSES modification of K95C ($P < 0.005$), and daggers indicate a significant difference from MTSES modification of the same mutant ($P < 0.05$). Mean of data from three patches in each case is shown.

MTSET to the intracellular solution. In fact, as shown quantitatively in Fig. 4 B, these currents showed indistinguishable sensitivity to intracellular MTSET to those recorded from patches excised from cells that had not been pretreated with extracellular MTSET (see, for example, Fig. 1). These results suggest that none of K95C, Q98C, P99C, or L102C can be modified covalently by extracellular MTSET.

Our work concerning intracellular MTS reagent modification in TM6 also identified some cysteines that could be modified in both activated and nonactivated channels (e.g., V345C and M348C), and others that could apparently be modified only after channel activation (e.g., T338C, S341C, and I344C), suggesting a state-dependent conformational change that alters access of internally applied MTS reagents into the pore (El Hiani and Linsdell, 2010). This difference was most readily apparent using a pretreatment protocol, in which cysteines introduced at some sites were modified by pretreatment of inside-out patches with intracellular MTSES, whereas others were apparently not modified unless the pretreatment also included PKA and ATP to promote channel activation (El Hiani and Linsdell, 2010). We used a similar approach to determine if K95C, Q98C, P99C, and L102C could be modified by MTSES pretreatment. Each of these mutants is rapidly modified by the application of 200 µM of intracellular MTSES applied after channel activation (Fig. 3), leading to a decrease in macroscopic current amplitude (Figs. 1 and 2). Fig. 5 (A and B) shows the effects of MTSES application under similar conditions to those in Fig. 1, after maximal channel stimulation with PKA, ATP, and PPi, but in inside-out patches that had been pretreated with 200 µM of intracellular MTSES (for a 2-min pretreatment period) under two different sets of pretreatment conditions (see Materials and methods). In Fig. 5 A, patches were pretreated with MTSES in the presence of PKA and ATP after patch excision, whereas in Fig. 5 B, inside-out patches were pretreated with MTSES alone. In this way, we expect MTSES applied during the pretreatment period to have access to activated channels in Fig. 5 A, but only to nonactivated channels in Fig. 5 B. In both cases, after the 2-min pretreatment period, all drugs were thoroughly washed from the bath, and channels were activated by PKA, ATP, and PPi before the application of a second test exposure to MTSES. In patches that had been pretreated with MTSES, PKA, and ATP and then washed, currents carried by each of these four mutants were insensitive to the second test exposure to MTSES (Fig. 5 A), suggesting that channels had been covalently modified by MTSES during the pretreatment period, and that this modification had not been reversed by washing the MTSES from the bath. However, different results were obtained when patches were pretreated with MTSES in the absence of PKA and ATP. Whereas K95C channels were again rendered insensitive to a test exposure to MTSES, again consistent with them having been covalently modified during pretreatment, currents carried by Q98C, P99C,

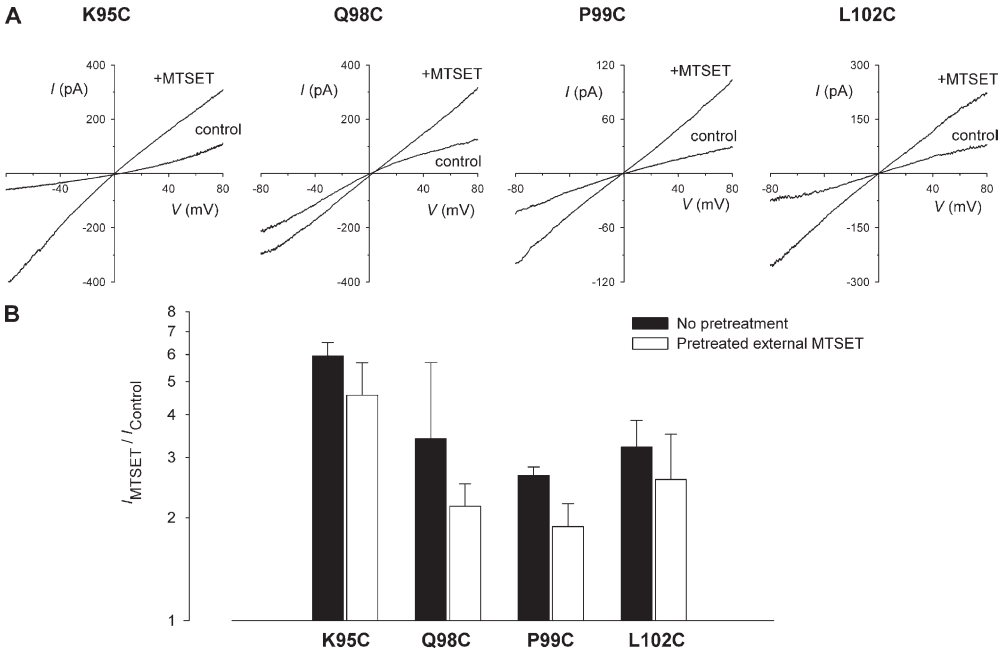

Figure 4. Modification of introduced cysteines by pretreatment with external MTSET. (A) Example leak-subtracted I-V relationships for each of the four MTSET-sensitive mutants named, showing the effects of the application of internal MTSET (2 mM) after maximal channel activation with 20 nM PKA, 1 mM ATP, and 2 mM PPi. Patches were excised from cells that had been pretreated with external MTSET (5 mM for 5 min) and showed similar sensitivity to internal MTSET as patches excised from untreated cells (see Fig. 1 B for examples). (B) Comparison of the effects of MTSET on macroscopic current amplitude at −80 mV between patches from untreated cells and patches from cells pretreated with external MTSET. There were no statistically significant differences for any mutant studied ($P > 0.05$). Mean of data from three to nine patches is shown.

and L102C were all strongly inhibited by the application of the test dose of MTSES, suggesting that they were not covalently modified by MTSES pretreatment. These results, which are summarized quantitatively in Fig. 5 C, suggest that although K95C can be modified by MTSES before channel activation, Q98C, P99C, and L102C are modified by MTSES only very slowly, if at all, in channels that have not been activated by PKA and ATP.

Proximity and alignment of TMs 1 and 6

The results described in Fig. 5, suggesting that K95C is accessible to cytoplasmic MTSES in nonactivated channels but that Q98C is accessible only in activated channels, imply that K95 and Q98 may lie close to the putative barrier within the pore that we recently proposed to regulate access from the cytoplasmic solution (El Hiani and Linsdell, 2010). In TM6, I344 and V345 were proposed to lie on either side of this barrier, based on similar

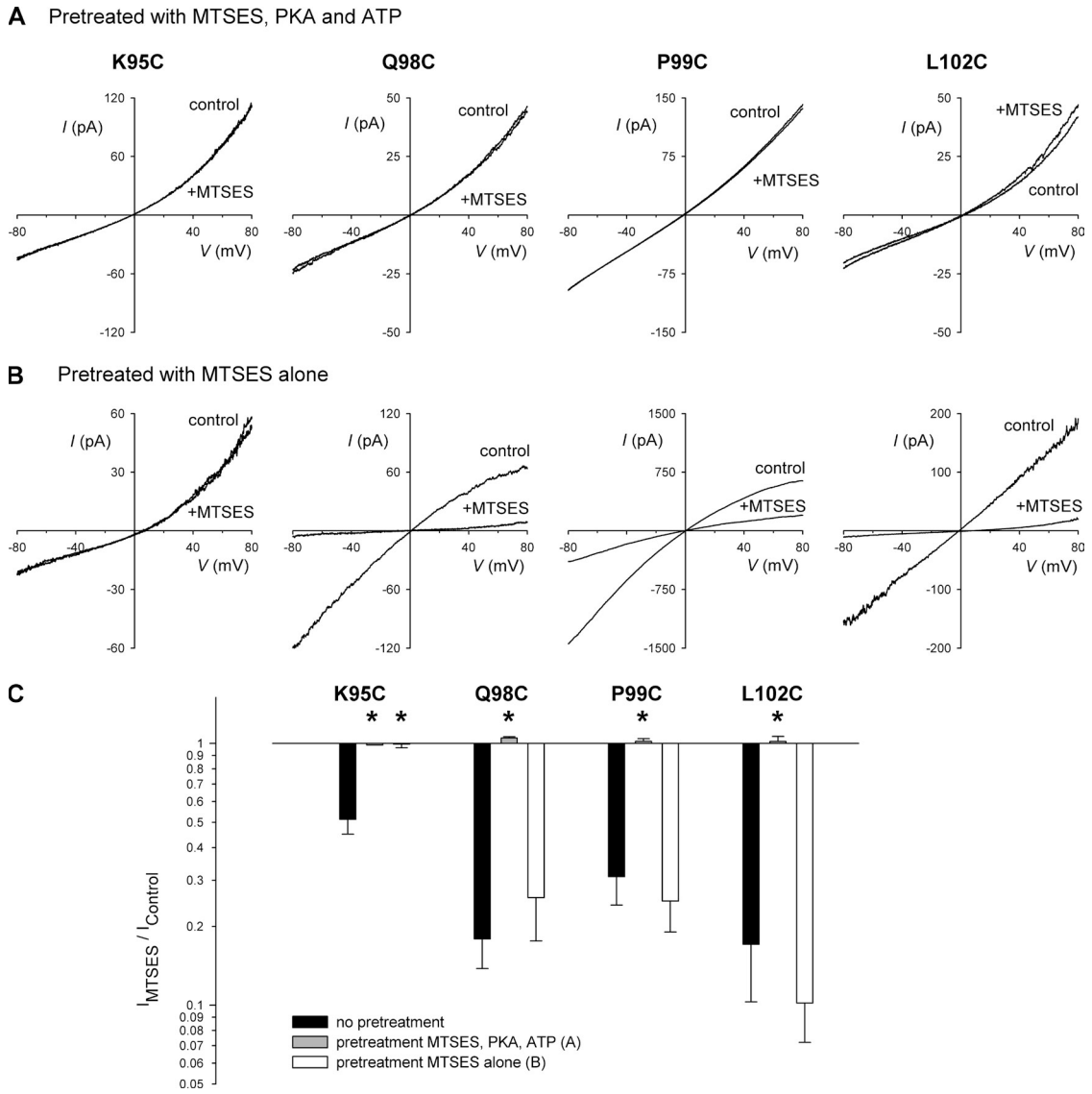

Figure 5. Modification of introduced cysteines during pretreatment with internal MTSES. (A and B) Example leak-subtracted I-V relationships for each of the four MTSES-sensitive mutants named, showing the effects of the application of internal MTSES (200 µM) after maximal channel activation with 20 nM PKA, 1 mM ATP, and 2 mM PPi. Patches have been pretreated in two different ways (see Materials and methods): (A) pretreated with 200 µM MTSES, PKA, and ATP for 2 min; (B) pretreated with 200 µM MTSES alone for 2 min. Similar examples for patches that underwent no pretreatment are shown in Fig. 1 B. Note that for each mutant, after pretreatment with MTSES, PKA, and ATP, stimulated currents appeared refractory to the effects of internally applied MTSES (A), suggesting that channels had been covalently modified during the pretreatment. (C) Mean effect of internal MTSES on macroscopic current amplitude at +80 mV under three different sets of condition as indicated: no pretreatment (see Fig. 1 B); pretreated with MTSES, PKA, and ATP (A); and pretreated with MTSES alone (B). Asterisks indicate a significant difference from control (no pretreatment) conditions ($P < 0.005$); other groups not marked by an asterisk showed no significant difference from control conditions ($P > 0.3$). Mean of data from three to six patches is shown.

apparent state-dependent changes in accessibility to intracellular MTSES (El Hiani and Linsdell, 2010). Furthermore, the MTSES modification rate constants for cysteines introduced at these four sites (K95, Q98, I344, and V345) were similar, whereas those for cysteines introduced closer to the outer ends of TM1 (P99 and L102) or TM6 (T338 and S341) were considerably lower (Fig. 3) (El Hiani and Linsdell, 2010) (see Discussion). We therefore speculated that K95 and Q98 in TM1 might be located close to I344 and V345 in TM6 in the three-dimensional structure of the CFTR pore, perhaps being situated around a regulated barrier to ion movement in nonactivated channels. To test this idea, we therefore used site-directed mutagenesis to create

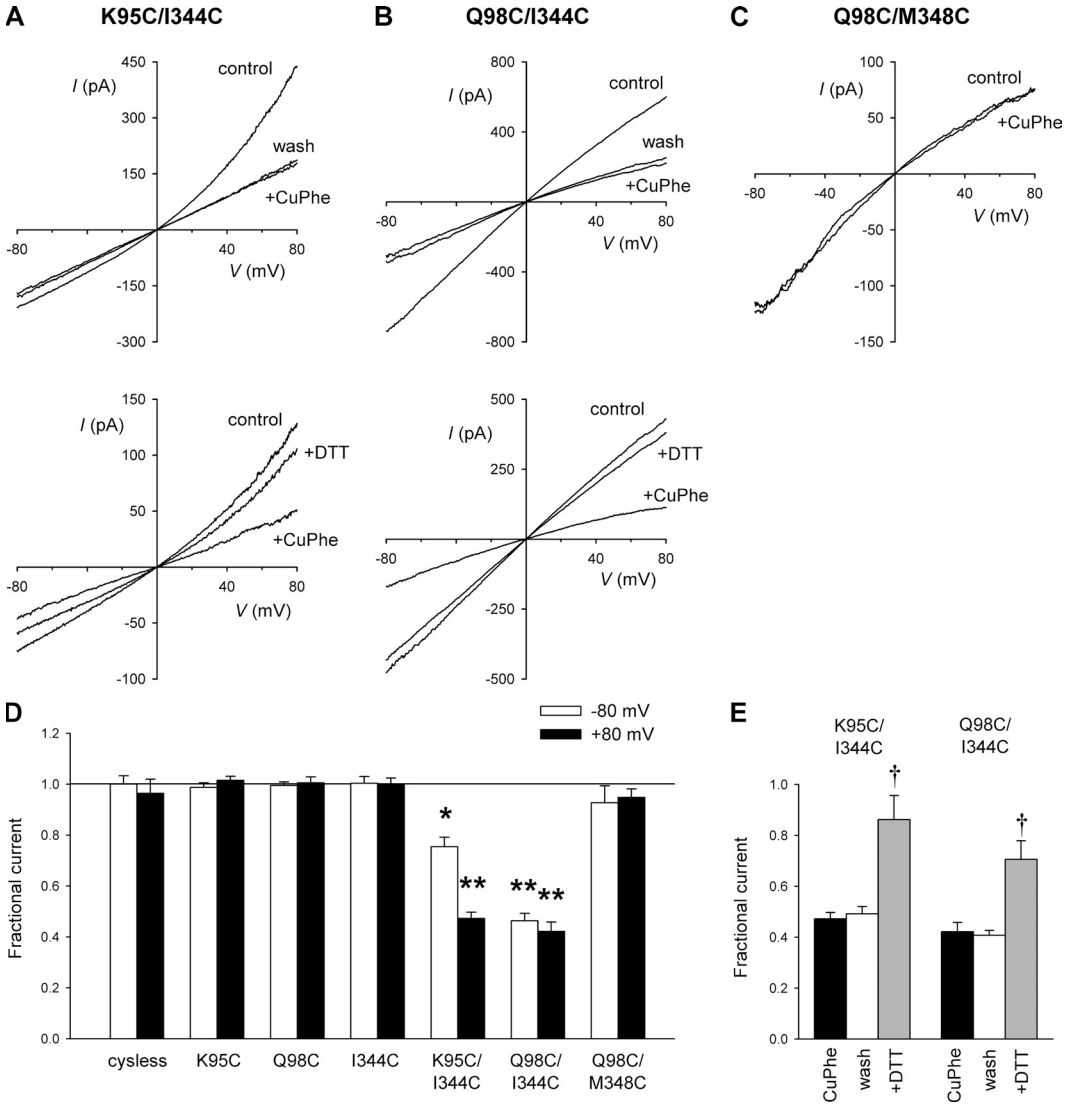

Figure 6. Cross-linking of TMs 1 and 6 by the oxidizing agent CuPhe. (A–C) Example leak-subtracted I-V relationships for K95C/I344C (A), Q98C/I344C (B), and Q98C/M348C (C) after channel activation with 20 nM PKA and 1 mM ATP. In A and B, current amplitude is decreased by the subsequent addition of CuPhe to the intracellular solution, whereas in C, CuPhe is without effect. In both CuPhe-sensitive channel constructs, the inhibitory effects of CuPhe were not reversed by washing CuPhe from the bath (top panels in both A and B), but were reversed by the addition of 5 mM DTT to the intracellular solution (bottom panels in both A and B). (D) Mean effect of internal CuPhe on macroscopic current amplitude under these conditions, measured at membrane potentials of −80 mV (white bars) and +80 mV (black bars). Note that cys-less CFTR, the single mutants K95C, Q98C, or I344C, and the double mutant Q98C/M348C were all insensitive to CuPhe under these conditions. Also note that CuPhe had a stronger inhibitory effect on currents carried by K95C/I344C when measured at +80 mV compared with −80 mV; this same apparent voltage dependence was previously reported for K95C/S1141C under similar experimental conditions (Zhou et al., 2010). In contrast, the inhibitory effects of CuPhe on Q98C/I344C were similar when measured at −80 mV or +80 mV. Asterisks indicate a significant difference from control: *, $P < 0.005$; **, $P < 0.00005$. (E) Mean effects of CuPhe (black bars), CuPhe followed by washing with normal bath solution (white bars), and CuPhe followed by DTT (gray bars) on macroscopic current amplitude in K95C/I344C (left) and Q98C/I344C (right) at +80 mV. Daggers indicate a significant difference from CuPhe alone ($P < 0.005$); washing alone (white bars) had no significant effect compared with CuPhe alone ($P > 0.6$). Mean of data from three to seven patches is shown in D and E.

"paired" mutants with one cysteine introduced into each of TM1 (at K95 or Q98) and TM6 (at I344 and V345). Unfortunately, the double mutants K95C/V345C and Q98C/V345C did not yield functional currents when expressed in BHK cells, even after treatment with DTT to break any possible disulfide bonds; a similar lack of functional expression was previously reported for K95C/S341C (Zhou et al., 2010). However, K95C/I344C, Q98C/I344C, and Q98C/M348C did generate macroscopic PKA- and ATP-dependent currents in inside-out patches. These currents were not affected by the addition of 5 mM DTT to the intracellular solution (Fig. S2), suggesting that spontaneous disulfide bond formation between the two introduced cysteine side chains is either negligible, without functional consequence, or cannot be reversed by DTT. However, the oxidizing agent CuPhe, which has previously been used to induce disulfide bond formation between introduced cysteines in other parts of the CFTR protein (Mense et al., 2006; Loo et al., 2008; Serohijos et al., 2008; Zhou et al., 2010), led to a strong reduction in current amplitude in both K95C/I344C and Q98C/I344C (Fig. 6). Neither cys-less CFTR nor the single mutants K95C, Q98C, or I344C appeared sensitive to CuPhe under these conditions (Fig. 6 D), consistent with this agent acting by causing disulfide bond formation between the two introduced cysteine side chains in the double mutants K95C/I344C and Q98C/I344C. Furthermore, the lack of effect of CuPhe on Q98C/M348C indicated that not all double-cysteine mutants were CuPhe sensitive, which we take to indicate that only nearby cysteine side chains can be cross-linked by this reagent. Inhibition of both K95C/I344C and Q98C/I344C by CuPhe was not reversed by washing CuPhe from the bath; however, partial reversal was seen when 5 mM DTT was applied in the continued presence of CuPhe (Fig. 6, A, B, and E), consistent with CuPhe inhibition of these channels reflecting some oxidative process.

The results shown in Fig. 6 suggest that disulfide bond formation can occur between K95C and I344C and between Q98C and I344C after channel activation. To test whether these cysteines can also be cross-linked before channel activation, we used a CuPhe pretreatment protocol (Fig. 7). After patch excision, inside-out patches from cells expressing either K95C/I344C or Q98C/I344C were treated with cytoplasmic CuPhe for 2 min, after which CuPhe was washed from the bath and currents were activated using PKA and ATP, as usual. Currents activated in this way appeared normal and were not sensitive to the application of 5 mM DTT (Fig. 7), suggesting that negligible disulfide bond formation had taken place during the CuPhe pretreatment period. This contrasts with the robust DTT sensitivity of channels that had been treated with CuPhe after channel activation (Fig. 7 C), suggesting that disulfide bond formation had occurred under these conditions.

Both K95C/I344C and Q98C/I344C channel currents were also potently inhibited by the addition of Cu^{2+} ions alone (without phenanthroline) to the bath (Fig. 8). However, these effects were fully and easily reversed simply by washing the Cu^{2+} ions from the bath (Fig. 8 A), indicating that inhibition by Cu^{2+} was by a different mechanism than that by CuPhe. Each of the single mutants K95C, Q98C, and I344C showed reversible

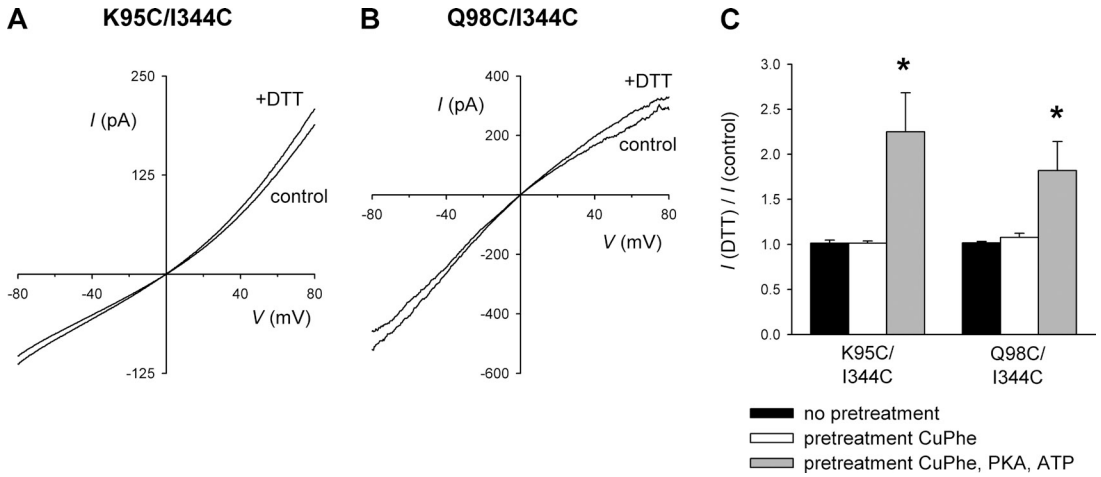

Figure 7. Insensitivity to CuPhe before channel activation. (A and B) Example leak-subtracted I-V relationships for K95C/I344C (A) and Q98C/I344C (B) after channel activation with 20 nM PKA and 1 mM ATP in inside-out patches that had been pretreated with CuPhe for 2 min, and then washed to remove CuPhe. Currents were recorded before (control) and after (+DTT) the addition of 5 mM DTT to the cytoplasmic solution. (C) Mean effect of DTT on current amplitude in patches that had never seen CuPhe (no pretreatment), had been pretreated as in A and B (pretreatment CuPhe), or had been treated with CuPhe after channel activation (pretreatment CuPhe, PKA, ATP). In these experiments, an increase in current amplitude after DTT application is taken as evidence that disulfide bond formation had taken place. Asterisks indicate a significant difference from no pretreatment conditions ($P < 0.05$). Mean of data from three to six patches is shown in C.

inhibition by Cu^{2+} that was of intermediate potency between the cys-less background and the double mutants K95C/I344C and Q98C/I344C. These results are consistent with the ability of metal ions such as Cu^{2+} to bind reversibly to cysteine side chains (Lippard and Berg, 1994). Nevertheless, the irreversible effects of CuPhe shown in Fig. 6 are clearly via a different mechanism and apparently not contaminated by the reversible inhibitory effects of free Cu^{2+} ions.

DISCUSSION

Structure and orientation of TM1

Previous functional (Anderson et al., 1991; Sheppard et al., 1996; Ge et al., 2004; Linsdell, 2005; Zhou et al., 2010) and substituted cysteine accessibility (Akabas et al., 1994) work has suggested that TM1 lines the CFTR pore and contributes to pore functional properties. Consistent with this, our present work shows that cysteines substituted for four different residues in TM1—K95, Q98, P99, and L102—are covalently modified by intracellularly applied MTSES and MTSET (Figs. 1 and 2). The positively charged side chain of K95 is well known to be involved in electrostatic attraction of Cl^- ions to the CFTR pore, and also contributes to interactions with cytoplasmic open-channel blocking anions (Linsdell, 2005; Zhou et al., 2010). Cysteine introduced at this position has also previously been shown to be modified by MTS reagents (Akabas et al., 1994; Zhou et al., 2010). The importance of this residue in the normal Cl^- permeation mechanism is demonstrated by the finding that mutations that remove the positive charge at this position drastically reduce unitary Cl^- conductance (Ge et al., 2004; Zhou et al., 2010). Mutagenesis of Q98 (Ge et al., 2004) and P99 (Sheppard et al., 1996; Ge et al., 2004) has also been shown to reduce unitary conductance. To our knowledge, the involvement of L102 has not previously been addressed by any mutagenesis study. At the outer end of TM1, another positively charged side chain, that of R104, is exposed to the extracellular solution where it acts to attract both Cl^- and blocking ions to the pore (Zhou et al., 2008). However, R104C was not sensitive to intracellularly applied MTS reagents (Figs. 1 and 2), consistent with the idea that such reagents are not able to permeate the CFTR pore (Alexander et al., 2009; El Hiani and Linsdell, 2010).

Our results concerning the accessibility of cysteines introduced into TM1 are summarized, and compared

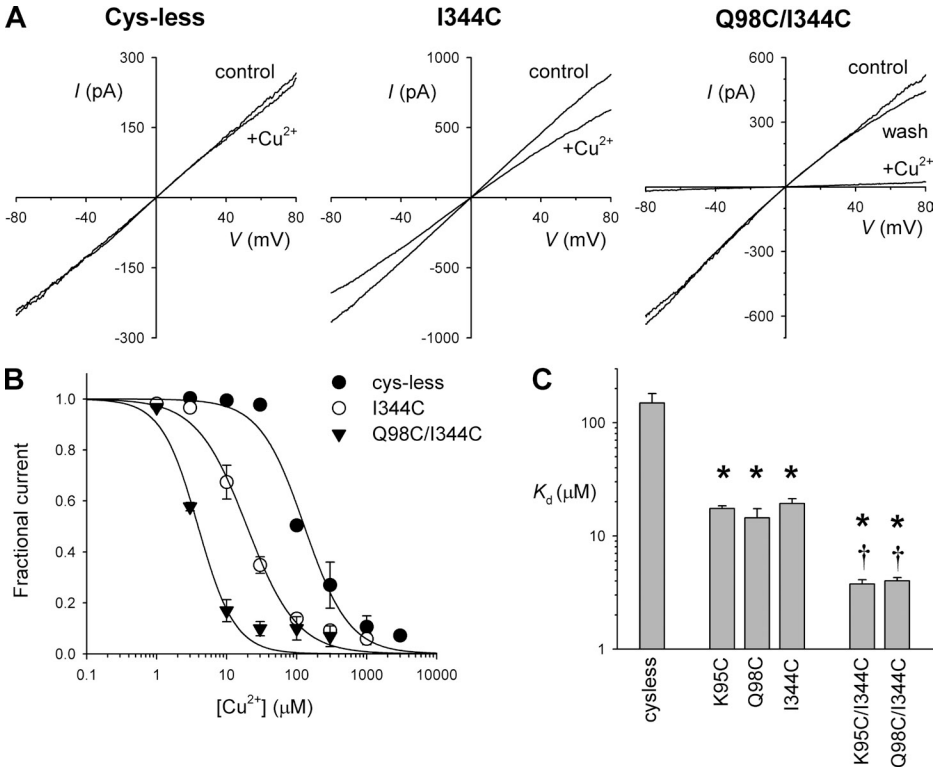

Figure 8. Reversible inhibition by cytoplasmic Cu^{2+} ions. (A) Example leak-subtracted I-V relationships for cys-less (left), I344C (center), and Q98C/I344C (right) after channel activation with 20 nM PKA and 1 mM ATP. In each panel, currents are shown before (control) and after the addition of 10 μM Cu^{2+} to the intracellular solution. In all channel constructs studied, these inhibitory effects of Cu^{2+} were readily and rapidly reversed by washing Cu^{2+} from the bath (for example, see right panel for complete reversal of the strong blocking effect on Q98C/I344C). (B) Mean fractional current remaining after the addition of different concentrations of Cu^{2+} for cys-less (●), I344C (○), and Q98C/I344C (▼). Data are fitted as described in Materials and methods, giving K_d = 129 μM and nH = 1.36 for cys-less, K_d = 19.5 μM and nH = 1.21 for I344C, and K_d = 3.91 μM and nH = 1.65 for Q98C/I344C. (C) Mean K_d calculated from individual patches using fits of the kind shown in B. Asterisks indicate a significant difference from cys-less, and daggers indicate a significant difference between the double mutant indicated and either of the individual mutations alone ($P < 0.05$ in each case). Mean of data from four to seven patches shown in B and C.

with our previous findings in TM6, in Fig. 9. Although both of these TM regions appear to be pore lining, there are interesting differences in their apparent contributions to the pore. First, only side chains in the outer part of TM1 are accessible to the pore lining in this model, whereas TM6 appears to contribute to the entire length of the TM pore. Thus, cysteines substituted for Y84, G85, I86, F87, L88, Y89, L90, G91, V93, and T94, closer to the cytoplasmic end of TM1, were not modified functionally by the application of either MTSES or MTSET (Figs. 2 and S1). The simplest interpretation of these negative results is that this part of TM1 does not line the aqueous lumen of the pore. However, because our experiments measure the functional consequences of MTS modification, rather than detecting modification directly by biochemical means, it is possible that modification of some side chains at the cytoplasmic end of TM1 does occur but is without functional effect. This might seem surprising, as MTS modification of the analogous part of TM6 has large effects on channel function that might reflect changes in both channel conductance and channel gating (Bai et al., 2010; El Hiani and Linsdell, 2010). Thus, if the cytoplasmic end of TM1 is accessible to cytoplasmic MTS reagents, the consistent lack of functional effect might mean that this part of TM1 is not closely associated with the permeation pathway for Cl^- ions. Second, whereas cysteines substituted for TM6 residues in the putative narrow pore region—F337C, T338C, and S341C—could be modified by both intracellular and extracellular MTS reagents (El Hiani and Linsdell, 2010), no residues that could be modified from both sides of the membrane were identified in TM1. Thus, the side chains of TM1 mutants K95C, Q98C, P99C, and L102C that we identified as accessible to MTS reagents applied from the inside (Fig. 2) were not accessible to MTSET applied to the outside (Fig. 4), whereas R104C, previously shown to be modified by external MTS reagents (Zhou et al., 2008), was not modified by internal MTSES or MTSET (Fig. 2).

Clearly, TMs 1 and 6 make different overall contributions to the pore, with TM1 apparently contributing only to the outer part of the TM Cl^- permeation pathway. It is possible that although some TMs (such as TM6) contribute to the entire length of the pore, the contribution of other TMs varies along the axis of the pore. For example, we previously suggested that TM5 might make a greater functional contribution to the inner compared with the outer part of the pore (St. Aubin and Linsdell, 2006). Although it can be difficult to reconcile functional data with current atomic models of the CFTR pore region (Bai et al., 2010; El Hiani and Linsdell, 2010; Zhou et al., 2010; see below), such a model that is based on homology modeling of the bacterial ABC protein Sav1866 may offer one potential explanation for the differential contribution of different parts of TM1 to the pore. In this model, TM6 appears to lie parallel to the central axis of the pore, whereas TM1 appears bent, with its outer part lining the pore and its inner part pointing away from the pore and toward the outside of the membrane-spanning part of the CFTR protein (Mornon et al., 2008; Serohijos et al., 2008).

In open CFTR channels, internally applied MTS reagents can penetrate far enough into the pore as to modify L102C in TM1 and F337C in TM6. That MTS reagents are not permeant in CFTR (see above) suggests that some restriction in the open-channel pore prevents intracellularly applied MTS reagents from penetrating beyond these residues (Fig. 9). One possible explanation is that these residues lie close to the narrowest part of the pore. Interestingly, amino acid side chains only one to two residues closer to the outer ends of these TMs, R104C in TM1 and I336C in TM6, can be modified by external, but not internal, MTS reagents (Fig. 9). Thus, in TM1 the cutoff between the "outside" and "inside" parts of the pore appears very distinct between L102 and R104. In TM6, the boundary between outside and inside parts of the pore is less distinct, as there are three sites at which cysteine residues were found to be modified

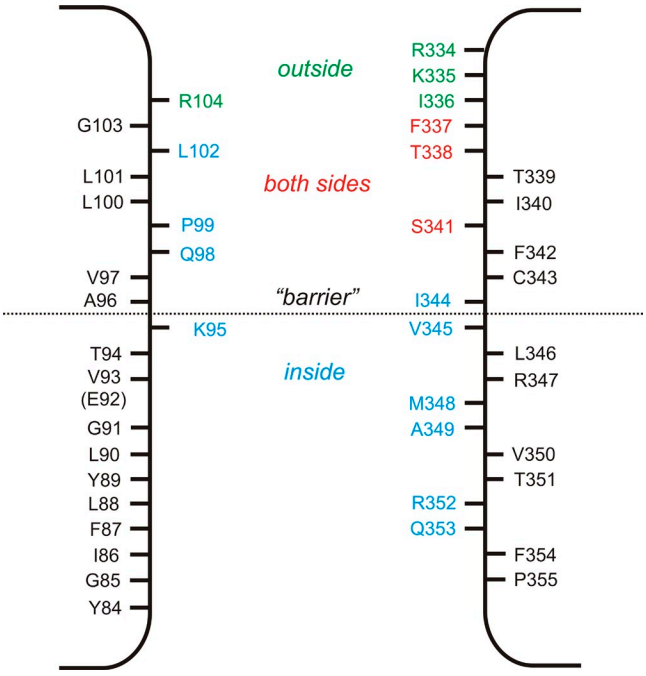

Figure 9. Proposed locations of pore-lining side chains in TM1 and TM6. Location of residues that, when mutated to cysteine, are exposed to intracellular MTS reagents only (blue), to extracellular MTS reagents only (green), or to MTS reagents applied to either side of the membrane (red) (see also El Hiani and Linsdell, 2010). Other residues that we find not to be modified by intracellular MTS reagents and are presumed to be non–pore lining are shown in black. For TM1 (left), internal MTS modification is as shown in Fig. 2; external MTS modification is as defined in Fig. 4 or in previous work (Zhou et al., 2008). For TM6 (right), the model is as presented previously (El Hiani and Linsdell, 2010).

by MTS reagents applied to either side of the membrane using approaches similar to those used in the present study (El Hiani and Linsdell, 2010) (Fig. 9). Currently, it is not clear why there are no sites in TM1 that can be accessed from both sides of the membrane in our hands (although it should be noted that Q98C was described as being sensitive to external MTSES in a previous study; Akabas et al., 1994). One possibility raised previously (El Hiani and Linsdell, 2010) is that TM6 undergoes some conformational change that allows it to be accessible to the outside in one conformation and the inside in another conformation. If this were the case, it would have to be postulated that TM1 does not show similar conformational movements, another potential functional difference between these two pore-forming helices.

The MTS reagent modification rate constant was greater for cysteines introduced closer to the intracellular end of TM1 (Fig. 3), suggesting that, even in open channels, some obstacle restricts the access of intracellular MTS reagents into the deeper reaches of the pore. A similar restriction to MTSES modification was seen in TM6 (El Hiani and Linsdell, 2010) and was proposed to represent a physical narrowing of the pore lumen. For comparison, the MTSES modification rate constant for P99C and L102C (Fig. 3) was similar to that of T338C and S341C in TM6 (El Hiani and Linsdell, 2010) (all between 100 and 150 M^{-1} s^{-1}), and the modification rate constant for K95C was comparable to, or slightly greater than, that of I344C, V345C, and M348C (El Hiani and Linsdell, 2010) (all between 2,000 and 4,000 M^{-1} s^{-1}). These two "groups" of residues coming from two different TMs may therefore exist at regions inside the pore with approximately equivalent access to cytoplasmic MTSES (Fig. 9). The MTSES modification rate constant for Q98C (~440 M^{-1} s^{-1}; Fig. 3) was somewhat intermediate between these two groups. Interestingly, at each site investigated in TM1, the modification rate constant for MTSET was consistently ~8–13-fold lower than that for MTSES (Fig. 3). Because MTSES and MTSET are similar molecules, the most likely explanation for this difference in modification rate constant is that access to the anion-selective CFTR pore from the cytoplasm is easier for negatively charged MTSES than for positively charged MTSET. If this is the case, the similar discrepancy between MTSES and MTSET modification rate constants at all sites tested implies that the location of anion–cation discrimination that underlies this discrepancy may lie between the cytoplasmic mouth of the pore and the most accessible cysteine residue, namely, that at K95C. It has previously been suggested that the cytoplasmic mouth of the CFTR pore is a site that determines anion–cation selectivity (Guinamard and Akabas, 1999).

Previous work investigating state-dependent access of MTSES to cysteines introduced into TM6 suggested that a barrier exists inside the pore that prevents access of cytoplasmic substances in nonactivated channels (El Hiani and Linsdell, 2010). Although we have not investigated the state dependence of MTSES modification in TM1 in such great detail, our present results suggest a similar arrangement in which K95C can readily be modified before channel activation (Fig. 5), whereas Q98C, P99C, and L102C are modified rapidly after channel activation (Fig. 3) but very slowly if at all before activation (Fig. 5). We would therefore speculatively suggest that K95, like TM6 residues V345 and M348, exists on the cytoplasmic side of the putative barrier inside the pore, whereas Q98, P99, and L102, like T338, S341, and I344 in TM6, are located on the extracellular side of the barrier (Fig. 9).

Alignment of TMs 1 and 6

The model we have developed in Fig. 9, based on the functional effects of intracellular MTS reagents, suggests a relative alignment of pore-lining TMs 1 and 6. To test this proposed alignment functionally, we attempted to cross-link pore-lining cysteine side chains in these two TMs. Changes in channel function after the addition of the oxidizing agent CuPhe, that were not reversed by removal of this agent, were taken as evidence for the formation of a disulfide bridge between K95C in TM1 and I344C in TM6, and between Q98C in TM1 and I344C in TM6 (Fig. 6). Given that it is believed that the β-carbon distance must be in the range of ~5–8 Å for such disulfide bonds to form (Careaga and Falke, 1992), these results are consistent with close proximity of these pairs of pore-lining side chains in the three-dimensional structure of the pore. In contrast, we found no evidence for disulfide bond formation between a pair of introduced cysteine side chains that would be predicted (based on Fig. 9) to be further apart, Q98C in TM1 and M348C in TM6 (Fig. 6, C and D). These data therefore add support to the model shown in Fig. 9 and, by suggesting a close physical proximity of specific pore-lining amino acid side chains, extend this model of the CFTR pore into three dimensions. Furthermore, disulfide bond formation apparently required channel activation (Fig. 7), consistent with at least one of each pair of cysteine residues being located beyond the barrier and inaccessible to cytoplasmic reagents before channel activation (Fig. 9). The location of these putative neighboring side chains in an atomic homology model of the CFTR TM region is shown in Fig. S3.

Introduction of pore-lining cysteine side chains also increased channel sensitivity to inhibition by Cu^{2+} ions (Fig. 8). Although this is consistent with the known metal-binding properties of cysteine side chains, the completely reversible nature of inhibition by even high concentrations of Cu^{2+} (Fig. 8) indicates that this inhibitory effect did not contribute to the inhibitory effects of CuPhe (Fig. 6).

Three-dimensional structure of the pore

The functional effects of mutating individual pore-lining amino acids in CFTR have been described in great detail (see Introduction); however, it is difficult to put these findings into a three-dimensional context. Atomic homology models give a three-dimensional picture of the pore-forming TM region (Mornon et al., 2008, 2009; Serohijos et al., 2008); however, direct experimental evidence concerning the three-dimensional architecture of the pore is only beginning to emerge (Alexander et al., 2009; Zhou et al., 2010). CFTR has been modeled in the "outward-facing" conformation using the crystal structure of the bacterial ABC protein Sav1866 as a template (Mornon et al., 2008; Serohijos et al., 2008; Alexander et al., 2009), and in the "inward-facing" conformation from another bacterial ABC protein, MsbA (Mornon et al., 2009). It was suggested that the outward-facing conformation, in which the pore is open to the extracellular side of the membrane and constricted only at the cytoplasmic end of the TMs, represents the open state of the channel, whereas the inward-facing conformation, in which the TMs are much more parallel and closely associated, represents the closed state (Mornon et al., 2009). However, there are several major discrepancies between the outward-facing structure and the open-channel structure of CFTR suggested by our data and summarized in Fig. 9. In the Sav1866-based outward-facing model, residues in the narrow pore region and inner vestibule, including K95, Q98, P99, and L102, appear exposed to the extracellular solution, whereas our own work indicates that these residues are exposed to the intracellular, not extracellular, side of the membrane in open channels (Fig. 9). According to Fig. 9, there should be a physical barrier to the movement of large MTS reagents in the open channel located between L102 (on the intracellular side) and R104 (on the extracellular side), suggesting that the narrowest part of the open-channel pore is close to the extracellular side of the membrane. As previously discussed by Bai et al. (2010), these outward-facing models are also in conflict with long-standing functional data suggesting that the open-channel pore has a deep and wide inner vestibule that is open to the cytoplasm (Linsdell, 2006). Furthermore, our suggestion that the channel is gated by a barrier at the level of K95/Q98/I344/V345, between the inner vestibule and narrow pore region (Fig. 9) (El Hiani and Linsdell, 2010), would seem to suggest that channel opening is associated with a physical widening in this part of the pore, cytoplasmic to the narrow pore region. Although much remains to be learned concerning the structure of the pore in the open and closed states, there are clear caveats to a simple designation of the outward-facing conformation as open and the inward-facing conformation as closed.

Our data provide important new information on the relative positions, functional contributions, and alignment of two important pore-lining TMs. This kind of information is necessary to develop and validate three-dimensional structural models of the pore region. Previously, we showed that a disulfide bond could be formed between K95C (in TM1) and S1141C (in TM12) (Zhou et al., 2010). Cysteine side chains can also be cross-linked between residues at the cytoplasmic ends of TM6 and TM12 (Chen et al., 2004), as well as between I340C (TM6) and S877C (TM7) (Wang et al., 2007); however, these findings are more difficult to interpret in structural terms because longer cross-linking molecules were used, and also because the side chain of I340C is not accessible to the aqueous lumen of the pore (Bai et al., 2010; El Hiani and Linsdell, 2010). Our present results suggest that both TM1 and TM6 contribute to the outer part of the pore and, at least at the level of K95/Q98/I344, come into close enough contact for disulfide bond formation to take place across the lumen of the pore (Figs. 9 and S3). In contrast, TM1 appears not to contribute to the inner part of the pore (Fig. 9), perhaps because this TM bends away from the central axis of the pore. Thus, the relative contribution of different TMs can vary along the length of the pore.

We would like to thank Drs. Feng Qian (Dalhousie University) and Xiandi Gong (University of Alberta) for sharing unpublished data.

This work was supported by the Canadian Institutes of Health Research and Cystic Fibrosis Canada (CFC). W. Wang is a CFC postdoctoral fellow.

Angus C. Nairn served as editor.

Submitted: 26 January 2011
Accepted: 22 June 2011

REFERENCES

Akabas, M.H., C. Kaufmann, T.A. Cook, and P. Archdeacon. 1994. Amino acid residues lining the chloride channel of the cystic fibrosis transmembrane conductance regulator. *J. Biol. Chem.* 269: 14865–14868.

Alexander, C., A. Ivetac, X. Liu, Y. Norimatsu, J.R. Serrano, A. Landstrom, M. Sansom, and D.C. Dawson. 2009. Cystic fibrosis transmembrane conductance regulator: using differential reactivity toward channel-permeant and channel-impermeant thiol-reactive probes to test a molecular model for the pore. *Biochemistry.* 48:10078–10088. doi:10.1021/bi901314c

Anderson, M.P., R.J. Gregory, S. Thompson, D.W. Souza, S. Paul, R.C. Mulligan, A.E. Smith, and M.J. Welsh. 1991. Demonstration that CFTR is a chloride channel by alteration of its anion selectivity. *Science.* 253:202–205. doi:10.1126/science.1712984

Bai, Y., M. Li, and T.-C. Hwang. 2010. Dual roles of the sixth transmembrane segment of the CFTR chloride channel in gating and permeation. *J. Gen. Physiol.* 136:293–309. doi:10.1085/jgp.201010480

Beck, E.J., Y. Yang, S. Yaemsiri, and V. Raghuram. 2008. Conformational changes in a pore-lining helix coupled to cystic fibrosis transmembrane conductance regulator channel gating. *J. Biol. Chem.* 283:4957–4966. doi:10.1074/jbc.M702235200

Careaga, C.L., and J.J. Falke. 1992. Structure and dynamics of *Escherichia coli* chemosensory receptors. Engineered sulfhydryl studies. *Biophys. J.* 62:209–216. doi:10.1016/S0006-3495(92)81806-4

Chen, E.Y., M.C. Bartlett, T.W. Loo, and D.M. Clarke. 2004. The DeltaF508 mutation disrupts packing of the transmembrane

segments of the cystic fibrosis transmembrane conductance regulator. *J. Biol. Chem.* 279:39620–39627. doi:10.1074/jbc.M407887200

Cheung, M., and M.H. Akabas. 1996. Identification of cystic fibrosis transmembrane conductance regulator channel-lining residues in and flanking the M6 membrane-spanning segment. *Biophys. J.* 70:2688–2695. doi:10.1016/S0006-3495(96)79838-7

El Hiani, Y., and P. Linsdell. 2010. Changes in accessibility of cytoplasmic substances to the pore associated with activation of the cystic fibrosis transmembrane conductance regulator chloride channel. *J. Biol. Chem.* 285:32126–32140. doi:10.1074/jbc.M110.113332

Fatehi, M., and P. Linsdell. 2008. State-dependent access of anions to the cystic fibrosis transmembrane conductance regulator chloride channel pore. *J. Biol. Chem.* 283:6102–6109. doi:10.1074/jbc.M707736200

Fatehi, M., and P. Linsdell. 2009. Novel residues lining the CFTR chloride channel pore identified by functional modification of introduced cysteines. *J. Membr. Biol.* 228:151–164. doi:10.1007/s00232-009-9167-3

Gadsby, D.C., P. Vergani, and L. Csanády. 2006. The ABC protein turned chloride channel whose failure causes cystic fibrosis. *Nature.* 440:477–483. doi:10.1038/nature04712

Ge, N., C.N. Muise, X. Gong, and P. Linsdell. 2004. Direct comparison of the functional roles played by different transmembrane regions in the cystic fibrosis transmembrane conductance regulator chloride channel pore. *J. Biol. Chem.* 279:55283–55289. doi:10.1074/jbc.M411935200

Gong, X., and P. Linsdell. 2003. Mutation-induced blocker permeability and multiion block of the CFTR chloride channel pore. *J. Gen. Physiol.* 122:673–687. doi:10.1085/jgp.200308889

Gong, X., S.M. Burbridge, E.A. Cowley, and P. Linsdell. 2002. Molecular determinants of $Au(CN)_2^-$ binding and permeability within the cystic fibrosis transmembrane conductance regulator Cl^- channel pore. *J. Physiol.* 540:39–47. doi:10.1113/jphysiol.2001.013235

Guinamard, R., and M.H. Akabas. 1999. Arg352 is a major determinant of charge selectivity in the cystic fibrosis transmembrane conductance regulator chloride channel. *Biochemistry.* 38:5528–5537. doi:10.1021/bi990155n

Kidd, J.F., I. Kogan, and C.E. Bear. 2004. Molecular basis for the chloride channel activity of cystic fibrosis transmembrane conductance regulator and the consequences of disease-causing mutations. *Curr. Top. Dev. Biol.* 60:215–249. doi:10.1016/S0070-2153(04)60007-X

Li, M.-S., A.F.A. Demsey, J. Qi, and P. Linsdell. 2009. Cysteine-independent inhibition of the CFTR chloride channel by the cysteine-reactive reagent sodium (2-sulphonatoethyl) methanethiosulphonate. *Br. J. Pharmacol.* 157:1065–1071. doi:10.1111/j.1476-5381.2009.00258.x

Linsdell, P. 2005. Location of a common inhibitor binding site in the cytoplasmic vestibule of the cystic fibrosis transmembrane conductance regulator chloride channel pore. *J. Biol. Chem.* 280:8945–8950. doi:10.1074/jbc.M414354200

Linsdell, P. 2006. Mechanism of chloride permeation in the cystic fibrosis transmembrane conductance regulator chloride channel. *Exp. Physiol.* 91:123–129. doi:10.1113/expphysiol.2005.031757

Linsdell, P., and X. Gong. 2002. Multiple inhibitory effects of $Au(CN)_2^-$ ions on cystic fibrosis transmembrane conductance regulator Cl^- channel currents. *J. Physiol.* 540:29–38. doi:10.1113/jphysiol.2001.013234

Linsdell, P., and J.W. Hanrahan. 1996. Disulphonic stilbene block of cystic fibrosis transmembrane conductance regulator Cl^- channels expressed in a mammalian cell line and its regulation by a critical pore residue. *J. Physiol.* 496:687–693.

Linsdell, P., and J.W. Hanrahan. 1998. Adenosine triphosphate–dependent asymmetry of anion permeation in the cystic fibrosis transmembrane conductance regulator chloride channel. *J. Gen. Physiol.* 111:601–614. doi:10.1085/jgp.111.4.601

Lippard, S.J., and J.M. Berg. 1994. Principles of Bioinorganic Chemistry. University Science Books, Mill Valley, CA. 417 pp.

Loo, T.W., M.C. Bartlett, and D.M. Clarke. 2008. Processing mutations disrupt interactions between the nucleotide binding and transmembrane domains of P-glycoprotein and the cystic fibrosis transmembrane conductance regulator (CFTR). *J. Biol. Chem.* 283:28190–28197. doi:10.1074/jbc.M805834200

McCarty, N.A. 2000. Permeation through the CFTR chloride channel. *J. Exp. Biol.* 203:1947–1962.

Mense, M., P. Vergani, D.M. White, G. Altberg, A.C. Nairn, and D.C. Gadsby. 2006. *In vivo* phosphorylation of CFTR promotes formation of a nucleotide-binding domain heterodimer. *EMBO J.* 25:4728–4739. doi:10.1038/sj.emboj.7601373

Mio, K., T. Ogura, M. Mio, H. Shimizu, T.-C. Hwang, C. Sato, and Y. Sohma. 2008. Three-dimensional reconstruction of human cystic fibrosis transmembrane conductance regulator chloride channel revealed an ellipsoidal structure with orifices beneath the putative transmembrane domain. *J. Biol. Chem.* 283:30300–30310. doi:10.1074/jbc.M803185200

Mornon, J.-P., P. Lehn, and I. Callebaut. 2008. Atomic model of human cystic fibrosis transmembrane conductance regulator: membrane-spanning domains and coupling interfaces. *Cell. Mol. Life Sci.* 65:2594–2612. doi:10.1007/s00018-008-8249-1

Mornon, J.-P., P. Lehn, and I. Callebaut. 2009. Molecular models of the open and closed states of the whole human CFTR protein. *Cell. Mol. Life Sci.* 66:3469–3486. doi:10.1007/s00018-009-0133-0

Rowe, S.M., S. Miller, and E.J. Sorscher. 2005. Cystic fibrosis. *N. Engl. J. Med.* 352:1992–2001. doi:10.1056/NEJMra043184

Serohijos, A.W.R., T. Hegedüs, A.A. Aleksandrov, L. He, L. Cui, N.V. Dokholyan, and J.R. Riordan. 2008. Phenylalanine-508 mediates a cytoplasmic-membrane domain contact in the CFTR 3D structure crucial to assembly and channel function. *Proc. Natl. Acad. Sci. USA.* 105:3256–3261. doi:10.1073/pnas.0800254105

Sheppard, D.N., S.M. Travis, H. Ishihara, and M.J. Welsh. 1996. Contribution of proline residues in the membrane-spanning domains of cystic fibrosis transmembrane conductance regulator to chloride channel function. *J. Biol. Chem.* 271:14995–15001. doi:10.1074/jbc.271.25.14995

St. Aubin, C.N., and P. Linsdell. 2006. Positive charges at the intracellular mouth of the pore regulate anion conduction in the CFTR chloride channel. *J. Gen. Physiol.* 128:535–545. doi:10.1085/jgp.200609516

Wang, Y., T.W. Loo, M.C. Bartlett, and D.M. Clarke. 2007. Correctors promote maturation of cystic fibrosis transmembrane conductance regulator (CFTR)-processing mutants by binding to the protein. *J. Biol. Chem.* 282:33247–33251. doi:10.1074/jbc.C700175200

Zhang, L., L.A. Aleksandrov, Z. Zhao, J.R. Birtley, J.R. Riordan, and R.C. Ford. 2009. Architecture of the cystic fibrosis transmembrane conductance regulator protein and structural changes associated with phosphorylation and nucleotide binding. *J. Struct. Biol.* 167:242–251. doi:10.1016/j.jsb.2009.06.004

Zhou, J.-J., M. Fatehi, and P. Linsdell. 2008. Identification of positive charges situated at the outer mouth of the CFTR chloride channel pore. *Pflugers Arch.* 457:351–360. doi:10.1007/s00424-008-0521-6

Zhou, J.-J., M.-S. Li, J. Qi, and P. Linsdell. 2010. Regulation of conductance by the number of fixed positive charges in the intracellular vestibule of the CFTR chloride channel pore. *J. Gen. Physiol.* 135:229–245. doi:10.1085/jgp.200910327